



Influence of Mesh Design and Surface Treatments on Particle Transport and Fate in a Vibration-Enhanced Flooded Bed Dust Scrubber

Mahmud Esad Uluer¹ · Aaron Noble¹

Received: 10 January 2024 / Accepted: 3 May 2024 / Published online: 23 May 2024
© The Author(s) 2024

Abstract

Respirable coal mine dust (RCMD) is one of the biggest occupational health hazards for underground coal miners. Dusty mining environments can cause long-term health problems, including pneumoconiosis and progressive massive fibrosis. The Mine Safety and Health Administration (MSHA) has recently revised regulations promoting enhanced dust mitigation technologies, which have sparked renewed interest in the development of dust mitigation technologies. The flooded bed dust scrubber (FBS) is one of the most widely used technologies; however, it is limited by technical challenges, the most notable being the potential to clog. Recent studies have shown that applying vibration to filter mesh can improve the overall efficiency of the scrubber and that the system can be readily integrated to existing continuous mining equipment using an energy harvesting approach. In this follow-up study, the impact of mesh design and surface modification on system efficiency was examined using different vibrating liquid-coated stainless-steel mesh panels in a laboratory-scale FBS. Based on the two-way interaction data from a multi-factor experimental design, the results show that the performance of the system can be optimized by using hydrophilic 20- or 30-layer filters and by excitation frequencies between 67 and 134 Hz. This laboratory study suggests that a 20-layer mesh screen with hydrophilic surface applications and optimized vibration parameters can perform similar to that of a 30-layer static mesh, which is typically used in industrial units.

Keywords Flooded bed dust scrubber · Continuous miner · Vibrating mesh filter · Surface modification · Filter density · Dust collection efficiency

1 Introduction

Respirable coal mine dust (RCMD) is one of the most significant occupational health hazards in the coal industry [1–5]. RCMD is defined as a particulate matter that has an aerodynamic diameter of below 10 μm and a median cut point of 4 μm [6]. It has been reported that this substance can be deposited anywhere along the lung's gas-exchange region [4]. According to recent research, smaller particles may pose more risk to health within their respirable range than larger particles [7]. In addition, technological advances in mining equipment have led to more powerful cutting, which, in turn, may cause smaller particles to be released into the mine area during the mining and drilling processes [8, 9].

Coal miners who work in dusty mining environments have been shown to suffer from long-term health effects, including but not limited to coal workers' pneumoconiosis (CWP) and progressive massive fibrosis (PMF) [10]. The Federal Coal Mine Health and Safety Act (Public Law 91-173) was enacted in 1969 to prevent the development of CWP in coal miners. It sets a limit at 2 mg/m^3 [11] for RCMD level with a minimum of 5% quartz. Regulations limiting respirable dust exposures, along with better ventilation and dust mitigation techniques, have contributed heavily to the decline in disease incidence in the US over the following several decades [4, 12–14]. However, since the late 1990s, the disease incidences have been on the rise [12, 14, 15] with some studies suggesting even 0.1–0.2 mg/m^3 exposure [6] can be harmful to the lungs. As a result of these issues, the Mine Safety and Health Administration (MSHA) implemented a new dust standard on August 1, 2016, requiring dust levels at the working face to remain below 1.5 mg/m^3 and intake entries below 0.5 mg/m^3 . Even though underground dust control has been the subject of research and inquiry for

✉ Mahmud Esad Uluer
esad@vt.edu

¹ Department of Mining and Minerals Engineering, Virginia Polytechnic Institute and State University, Blacksburg, VA 24061, USA

several decades, these revised regulations have prompted renewed interest in the area, particularly in the development of new technologies [16].

Dust control and mitigation strategies in modern mining include cutter-mounted sprays and dust scrubbers [17–22], while the ventilation system itself is also essential [23]. Augmenting these primary approaches, the flooded bed scrubber (FBS) mounted on the continuous mining machine is a widely adopted technology found in nearly all modern coal mines [24, 25]. The FBS works by drawing dirty air near the cutting head into a scrubbing duct. Here the dirty air passes through a mesh screen where water is continuously sprayed. The interaction of the water spray and mesh panel wets or captures the dust particles, which are subsequently captured in a mist eliminator. The dry clean air is then discharged at the rear of the machine where an exhaust fan induces the airflow needed for the scrubber [26]. Figure 1 shows a depiction of the FBS, with the slight adaptation of a vibration inducer that prompts controlled vibration to the mesh screen.

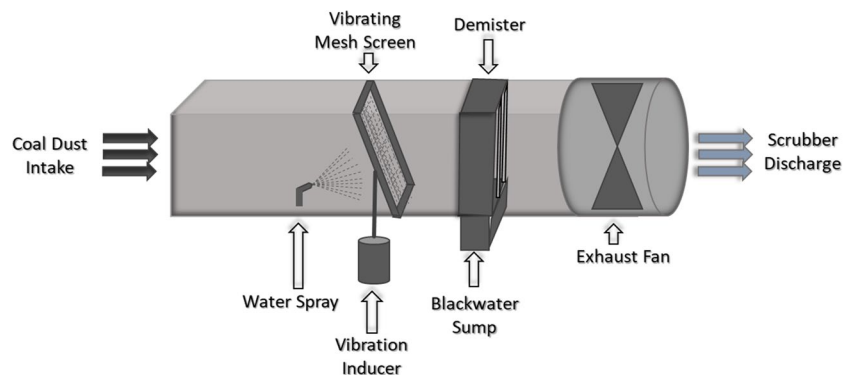
While FBSs are ubiquitously in continuous mining applications, they face numerous technical challenges. Most significantly, the units exhibit a fundamental tradeoff between airflow and mesh density. Higher mesh densities typically have higher particle capture rates; however, they also produce higher pressure drops, which reduce the amount of air that can be cleaned through the scrubber. Alternatively, low-density meshes can achieve higher air flow rates; however, the dust capture capacity is poor [26]. These issues are further compounded when the filter mesh is clogged, which reduces overall efficiency and necessitates frequent cleaning. At least one study shows that even a 20-foot advancement can reduce scrubber airflow by 35% [28]. Operational downtime caused by the cleaning process slows the production rate because of overall system degradation [29].

In recent years, research and development efforts have sought to directly address these challenges. In one example, a vortecone non-clogging wet filter used in the automobile industry to collect oversprayed vehicle paint particles [30] was used to replace the dust collector within the FBS [31]. Later, this structure was modified to minimize resistance

for use at much higher airflows [32]. In a separate study, researchers proposed an impingement-type filter facilitating dust removal by preventing the straight flow [33]. Recent attempts have been made to improve system performance by utilizing vibration-enhanced filter panels [27, 34, 35]. Many industrial applications have benefited from enhanced particle filtering using vibrating filter media, including size classification, filtering, and dust collection/removal [36–40]. It has also been shown that directly stimulating the filter media can reduce clogging problems in membrane filters [41, 42]. In-mine vibrational analysis on continuous miners' data exhibits peak acceleration levels occur around 100 Hz [43]. Additionally, the authors observed that the mesh screen responded with maximum vibrational energy when it excites in the range of 10–200 Hz [27].

Recent studies by the authors and colleagues have demonstrated the utility of vibration-enhanced FBS units. In an initial study, vibration-enhanced mesh panels were simulated through three-phase computational fluid dynamic (CFD) models [34, 35], and the results indicated that the vibrating mesh provides stronger dust particle-mesh interactions than the static mesh and that the strength of the interaction increases as vibrational energy increases, resulting in a greater level of dust collection. It was found that the lowest amplification values produced more particle collection than the higher values simulated. More recently, an experimental study validated that adding a vibration-enhanced mesh panel to a laboratory scale FBS can improve dust collection efficiency over that of a static unit by 6%. In that study, the system was also analyzed to investigate the size-by-size recovery of dust particles to various endpoints in the scrubber, under both vibrating and static conditions. Results show that while a majority of the particles are recovered into the demister sump, nearly a quarter of the dust mass is recovered upstream of the screen. In addition, the data confirm that vibration prompts notable improvements to collection efficiency, particularly particles with a diameter of less than 2.5 microns [27]. As a result of the induced vibration, more dust particles can be captured by water droplets, surface wetting can be improved, and airflow rates can be sustained

Fig. 1 Flooded bed scrubber [27]



for a longer period of time [27, 34, 35]. To implement the concept, energy harvesting approaches and specific spring configurations enable natural vibrations generated by continuous mining machines to be transmitted to mesh screen panels in FBSs [35, 44].

As a follow-up study of Uluer et al. [27], this study proposes further modifications to the standard FBS through surface modifications of the mesh filter. Many prior studies have evaluated the use of wetting agents and other modifications to the spray water; however, the results are largely inconsistent between studies and even within the same study [45–49]. In the current study, an alternative approach was applied, whereby the modification is applied to the filter media rather than the spray water. These surface modifications can increase adhesion between mine dust particles and liquid interfaces by increasing evenly wetting the mesh screen surface with liquid. A hydrophilic surface will enable water droplets to remain on the mesh for a longer period of time and thus allowing the drops to capture more dust particles. Hydrophobic surfaces will, however, enhance the rate of drop drainage, allowing droplets to continue their path to the mist eliminator. Considering these two competing effects, different coatings have been tested which provide a variety of surface wettability properties. Vibration-enhanced and surface-modified stainless-steel mesh panels with a variety of thicknesses were tested in this study to evaluate the combined effect of mesh design and surface modification on dust collection. For this purpose, several tests were conducted using a laboratory-scale FBS equipped with a vibration-enhanced mesh screen.

2 Materials and Methods

2.1 Testing Setup

The test setup used in this study is identical to that of Uluer et al. [27]. Salient details from that study are provided here for reader convenience.

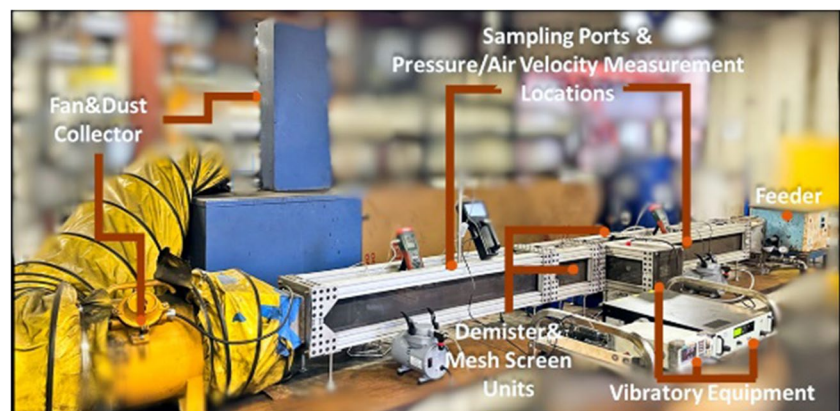
A bench-scale scrubber was manufactured by scaling down the parameters of a typical underground coal mine FBS. With an internal cross section of $0.152\text{ m} \times 0.152\text{ m}$, the chamber features a feeder, a jet mill grinder, an upwind section, a mesh screen unit, a shaker unit mounted on the side of the mesh screen unit, a demister unit, a downwind section, a fan, and a dust collector (Fig. 2). Both the upwind and downwind sections are 1.22 m long and have sampling stations for measuring air velocity and pressure. Each mesh screen and demister housing section is 0.36 m long, and both sections are equipped with grated blackwater sumps underneath. Through an actuating rod and clamping mechanism, the mesh screen was mounted to a Brüel and Kjær Type 4809 electromechanical shaker. SDG1000X function waveform generator generated the signals, which were applied to the shaker through a Brüel and Kjær Type 2718 power amplifier for base excitation (Fig. 3).

A volumetric screw feeder and a Trost jet mill are used to introduce dust material into the system. The two units are independent of one another and control dust size and concentration. This ensures that the dust introduced to the scrubber has fresh surfaces, as in a fully operational FBS. Keystone Black material obtained from Keystone Filler & Mfg. Co. was fed to the jet mill. This coal dust contains a low inherent moisture content of $1.4 \pm 0.10\%$ with a dry ash content of $14.6\% \pm 0.04\%$. 95% of the feed dust produced



Fig. 3 Vibratory instrument: waveform generator (left), power amplifier (middle), electro-mechanic shaker (right)

Fig. 2 Testing setup



by the jet mill passed approximately 10 microns and roughly 50% of it passed 5 mm microns. The dust material was selected because of its highly hydrophobic properties and high carbon content which mimics most RCMD materials. Air sampling cassettes preloaded with Teflon filters were used to collect dust samples from upwind and downwind sections during testing. As in the prior study, the particle size distribution of the samples was determined offline using a Microtrac S3500 laser particle size analyzer. Figure 4 shows the sampling ports positioned parallel to the incoming airstream at the chamber's centerline velocity.

2.2 Methodology

An efficiency study was conducted to determine the effects of vibrating filter panels with various mesh designs. Each test was conducted for 5 min, during which pressure drop and air velocity were continuously measured using pitot tubes, hot wire anemometers, and digital manometers to determine the level of mesh screen clogging. Each trial was conducted at an initial airspeed of approximately 9.5 m/s, and post-run air velocity measurements were taken to measure air velocity loss. Dust particles were introduced into the system at a rate of 22.7 g/min. The sampling pump flow rate was kept at 5 lt/min. Previously optimized parameters for water flow rate and vibrational parameters were used in the tests [27]. These values were respectively 3 lt/min for water flow rate, 30 dB for amplifier gain, and 134 Hz for frequency. These values were maintained throughout the test runs to ensure consistency in the experiments.

To ensure accurate and reliable measurements, various quality control and quality assurance measures were implemented during gravimetric sampling and analysis, with particular scrutiny in the pre- and post-filter sampling regions as well as other areas with relatively high airflow velocities. Prior to each test, all sampling and monitoring equipment, including pumps, flow/pressure meters, and filter holders, were calibrated to ensure accurate airflow measurement,

crucial for calculating dust deposition rates. To avoid bias, sampling locations within the wind tunnel were chosen where airflow velocities were relatively uniform and representative of the overall flow conditions. Areas near bends, junctions, or regions with turbulent flow were avoided, as these were anticipated to yield inaccurate sampling. During tests, the sampling duration was adjusted to accommodate the high airflow velocities and avoid both insufficient dust deposition (due to a short duration) and sample overloading (due to a long duration). Prior to data collection, exploratory tests were conducted to determine the appropriate sampling duration based on expected dust concentrations and airflow velocities. After each test, rigorous data validation procedures, including duplicate sampling and blank filter analysis, were implemented to ensure the accuracy and reliability of the gravimetric measurements. Lastly, the equipment design and study design were routinely assessed to ensure that the experiments focused on the particles of interest. Examples of these design parameters included feeding the system with known particle concentrations and size distributions under controlled conditions and routine leakage testing to eliminate the introduction or loss of unmeasured air.

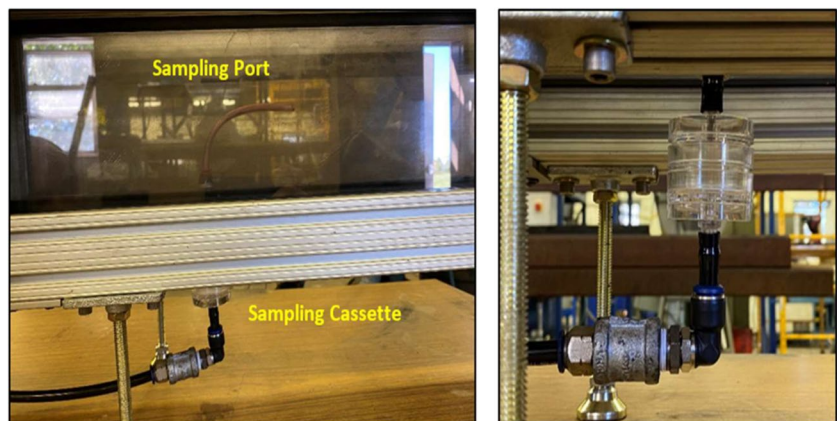
Dust collection efficiency was determined by gravimetrically collecting dust-laden air samples upwind and downwind of the filter assembly. Following is an equation for calculating the collection efficiency (η) associated with each individual test trial:

$$\eta (\%) = \left(1 - \frac{m_{ds}}{m_{us}} \right) * 100$$

m_{ds} = downstream sample weight, and m_{us} = upstream sample weight.

In addition to dust collection efficiency, mass accumulation within the mesh was also determined for each test. As discussed in Section 1, mass accumulation serves as a vital indicator of the filter's efficacy and excessive mass accumulation entails more frequent cleaning in an operating

Fig. 4 Gravimetric sampling system



environment. Thus, the ability to reduce mass accumulation while maintaining high dust removal efficiency is critical parameter influencing overall operability. This mass accumulation measurement was conducted by comparing the pre- and post-test filter weight following a meticulous and standardized cleaning and weighing procedure. Prior to each test, the clean filter weight was measured and recorded. After each test, the loaded filter was weighed again prior to cleaning. Initially, coarse particles were removed by hand and the filter was thoroughly sprayed with a water hose. Next, the filter was immersed in an ultrasonic bath for 3 min to dislodge and remove smaller adhered dust particles. Following the ultrasonic treatment, the mesh was dried in an oven to eliminate residual moisture and weighted again to confirm that the cleaning cycle was complete. This meticulous approach ensured consistent and reliable mass measurement results and preserved the mesh screen effectiveness in subsequent filtration assessments.

Customized filter frames were designed using a computer-aided design program and additively manufactured using a 3-D printer using the original mesh screen

dimensions (Fig. 5). In order to investigate how altered mesh design affects system performance, various layers of woven mesh and surface modifications were used. 10-layer, 20-layer, and 30-layer of 316 stainless steel woven mesh were used to fill the frames.

The performance of the system was also examined by testing modified screen chemistry with different surface treatments. The woven filter packages were made from 316 stainless steel with varying surface hydrophobicities. There are three types of screens: an untreated screen, a hydrophilic enhanced screen, and a hydrophobicized screen (Fig. 6). The bare steel had a contact angle of 92.6 ± 1.45 indicating that it was slightly hydrophobic [50]. Hydrophilic stainless steel meshes were made by heating them at $750\text{ }^\circ\text{C}$ for 20 min in a low-oxygen environment furnace. During this process, a blue magnetite layer formed on the surface. In response to this application, hydrophilic filters were produced by reducing the contact angle of bare steel to 37.1 ± 1.00 [50]. The superhydrophobic filters were produced by coating the bare steel meshes with a commercial polymer agent. This application increased the contact angle of the steel to 156.6 ± 0.88 [50].

Fig. 5 The mesh frame-adapter assembly is illustrated in **a** CAD drawing and **b** additively manufactured frames

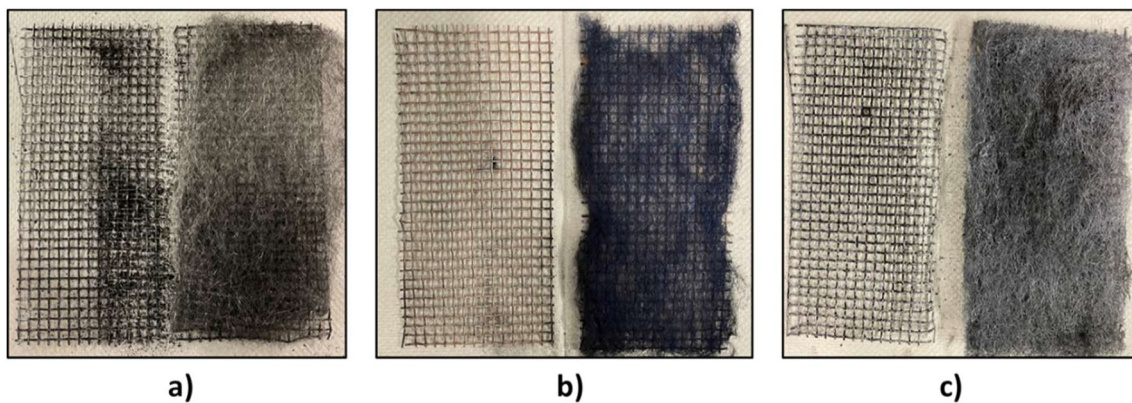
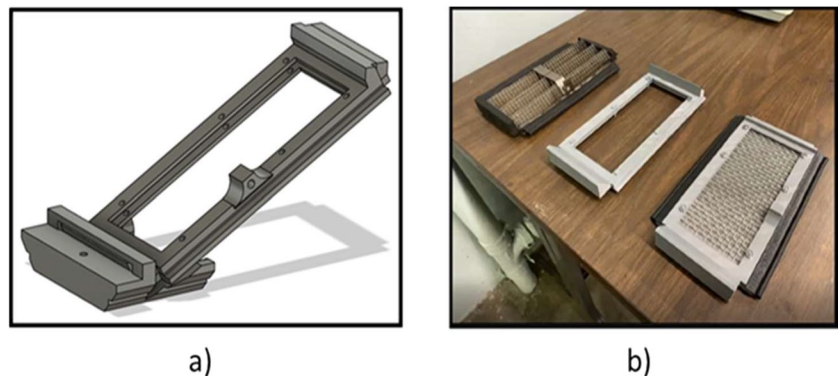


Fig. 6 Appearance of the screen after a trial. **a** Untreated (bare) screen. **b** Hydrophilic screen. **c** Hydrophobic screen

3 Results and Discussion

To evaluate the combined influence of mesh density and induced vibration on system efficiency, several tests were conducted using the bench-scale dust scrubber system. An in-house and purpose-built filter assembly was utilized to modify the filter package thickness (Fig. 5). In this trial, three separate mesh densities, namely, 30-layer, 20-layer, and 10-layer of woven stainless steel, were evaluated in both vibration-enhanced and vibration-free settings.

Dust collection efficiency data from these tests is shown in Fig. 7. The data obtained from the dust collection efficiency calculations showed that regardless of what filter package were used when the mesh screen is enhanced with the vibration, better results are obtained in both wet and dry conditions compared to the tests conducted in static condition. These differences are sometimes negligibly small for some operational conditions. However, an improvement of about 3.5% was obtained in the collection efficiency with the 30-layer screen in the wet vibration-enhanced operational condition compared to the same screen type under the wet vibration-free condition. The 30-layer wet vibration-enhanced operational condition was the most efficient run (92%). This is followed by the 30-layer wet vibration-free state with 89% efficiency. When each operational condition is evaluated in its own class, it will be seen that the lowest efficiency of that operational condition is always taking place with a 10-layer screen. The maximum achieved efficiency with

the 10-layer screen was under the wet vibration-enhanced operational condition (80%) and the lowest was about 77% under the dry vibration-free condition.

While collection efficiency is one evaluation metric, it must be considered alongside other metrics of performance. As such, throughout the same tests, the pre-test and post-test conditions of the downstream airflow were monitored. The difference of these two values shows how much air velocity loss occurs through the test duration. The greater the detected loss in air velocity implies greater mesh clogging and thus lowers the overall system efficiency. Data from this analysis is shown in Fig. 8. The highest air velocity loss occurred in the test with a dry and vibration-free operational condition with 30-layer screen (38.1%). The conditions with the least air loss were the tests with a 10-layer screen in each operational condition. The lowest air velocity loss occurred when a 10-layer mesh screen was used under the wet vibration-enhanced operational condition (8.2%).

As a supportive indicator to the air velocity loss parameter, the pressure difference data read digitally from the downstream and upstream directions of the system continuously throughout each run (Fig. 9). This data shows that the pressure in the wet condition tests always starts higher than the dry condition test, likely due to the water layer that coats the mesh and reduces mesh porosity. However, when the pressure change is monitored throughout the test, the data shows that the pressure changes in the tests performed under wet conditions are much less than the increase in pressure changes under dry conditions, because the initial pressure created by the water sprayed on the screen causes the initial

Fig. 7 Collection efficiency by different mesh screen packages with various filter layering under various operational modes

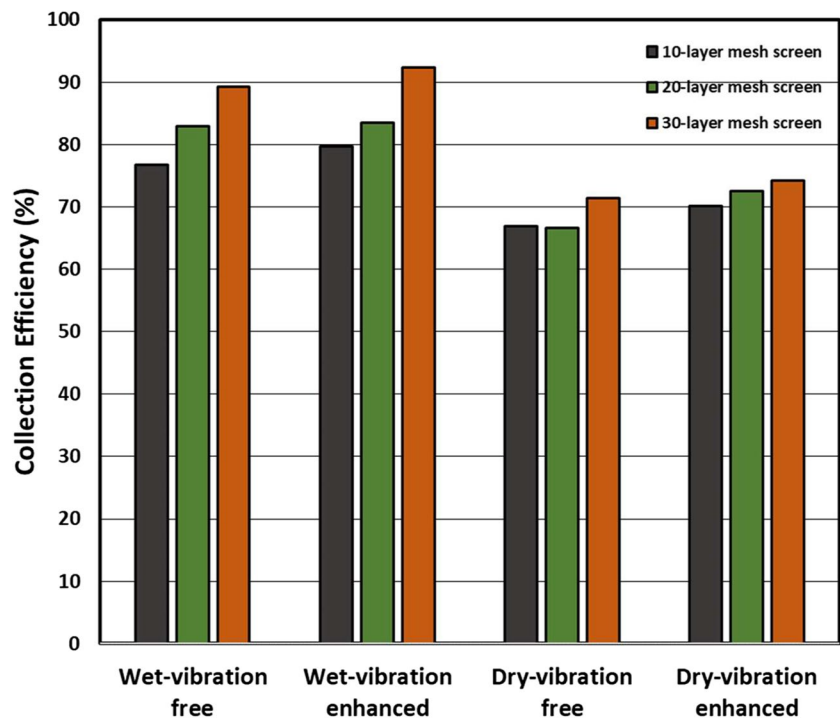
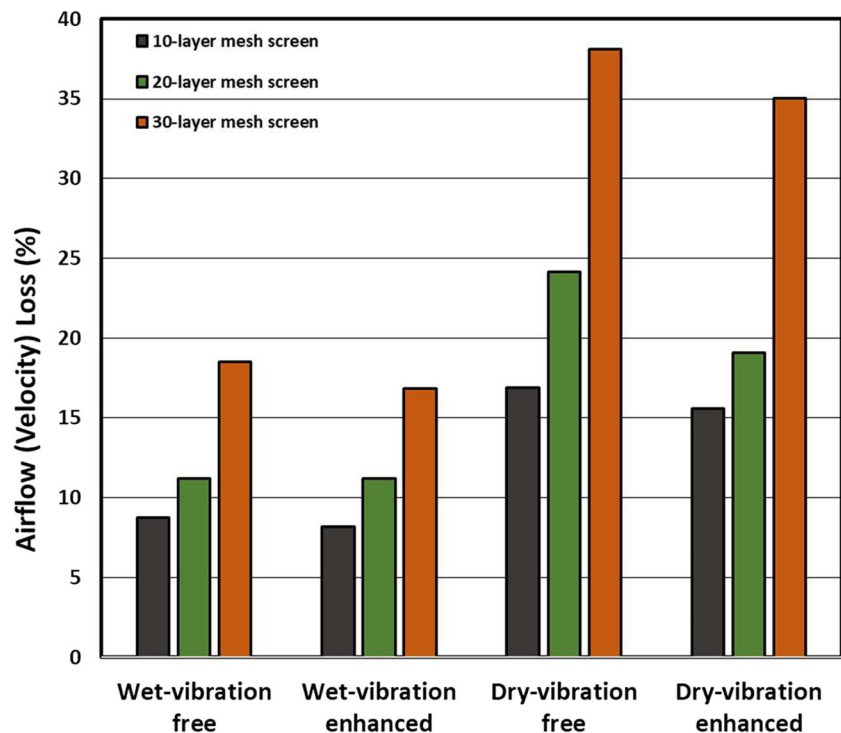


Fig. 8 Downwind section air velocity loss on mesh screen with different filter layering under various operational modes



pressure in the tests performed in wet conditions to start from high. The data show that the pressure difference in dry condition reaches much higher values (avg. 20% increase) than in wet condition (avg. 3.13% increase). The pressure drop increase throughout the test explains the partial clogging of the mesh screen. In the wet condition, no significant differences were observed in the vibrating and non-vibrating conditions. In addition, in each operational condition, the minimum increase in pressure difference was obtained in the tests performed with the 10-layer filter assembly under wet vibration-enhanced operational condition (2.2% increase), and the maximum pressure difference is obtained in the tests performed with the 30-layer filter assembly (22.4% increase).

In addition to these data, in order to further support the assessment of system efficiency, after each test, the filter assembly of that test was passed through an ultrasonic bath. The mass of material obtained from this procedure is indicative of the amount of dust accumulated on the filter during the test. This parameter is one of the most important parameters showing the clogging of the filter. As shown in Fig. 10, the operational condition in which the largest mass of particles accumulated on the filter during the test was the test with a 30-layer filter assembly under dry vibration-free condition (7.2 g). The operational condition where the least dust accumulation occurred on the mesh screen surface was the test with a vibrating 10-layer filter assembly under wet condition (2.9 g).

Although vibrating the mesh screen has been promising in many cases, it can be inferred from the combined data that there are a few situations where the static state is more advantageous. For example, while the air loss in the wet vibrating condition decreased by 7.78% compared to the vibration-free condition in the tests performed with the 30-layer mesh screen, the air velocity loss in the wet test using the 20-layer vibrating filter increased by 1.87% compared to the vibration-free condition. Similarly, a decrease of 4.77% is observed in the vibrating 30-layer screen under the wet condition compared to the vibration-free condition, while an increase of 9.14% is observed in the amount of dust accumulated on the filter surface with the vibrating 20-layer mesh screen compared to the vibration-free condition. When all these data are combined, the performance of the 10-layer screen is remarkable in terms of air loss and dust accumulation on the filter. However, when the system efficiency is also considered, significant decreases are observed in the 10-layer screen compared to the higher-layer filter packages in each operational situation. The reason for its less overall efficiency is that the dust-laden air passes the 10-layer filter screen without getting captured by water droplets more easily than others. Since less dense screens cause an increase in the amount of material that can move downstream of the system, they are negatively affecting the system efficiency.

When all the test results are considered together, the data show that the lowest air velocity and pressure loss and the lowest amount of mass accumulated on the screen

Fig. 9 Δp across mesh screen with different screen packages of **a** wet and vibration-free mode, **b** wet and vibration mode, **c** dry and vibration-free mode, and **d** dry and vibration mode

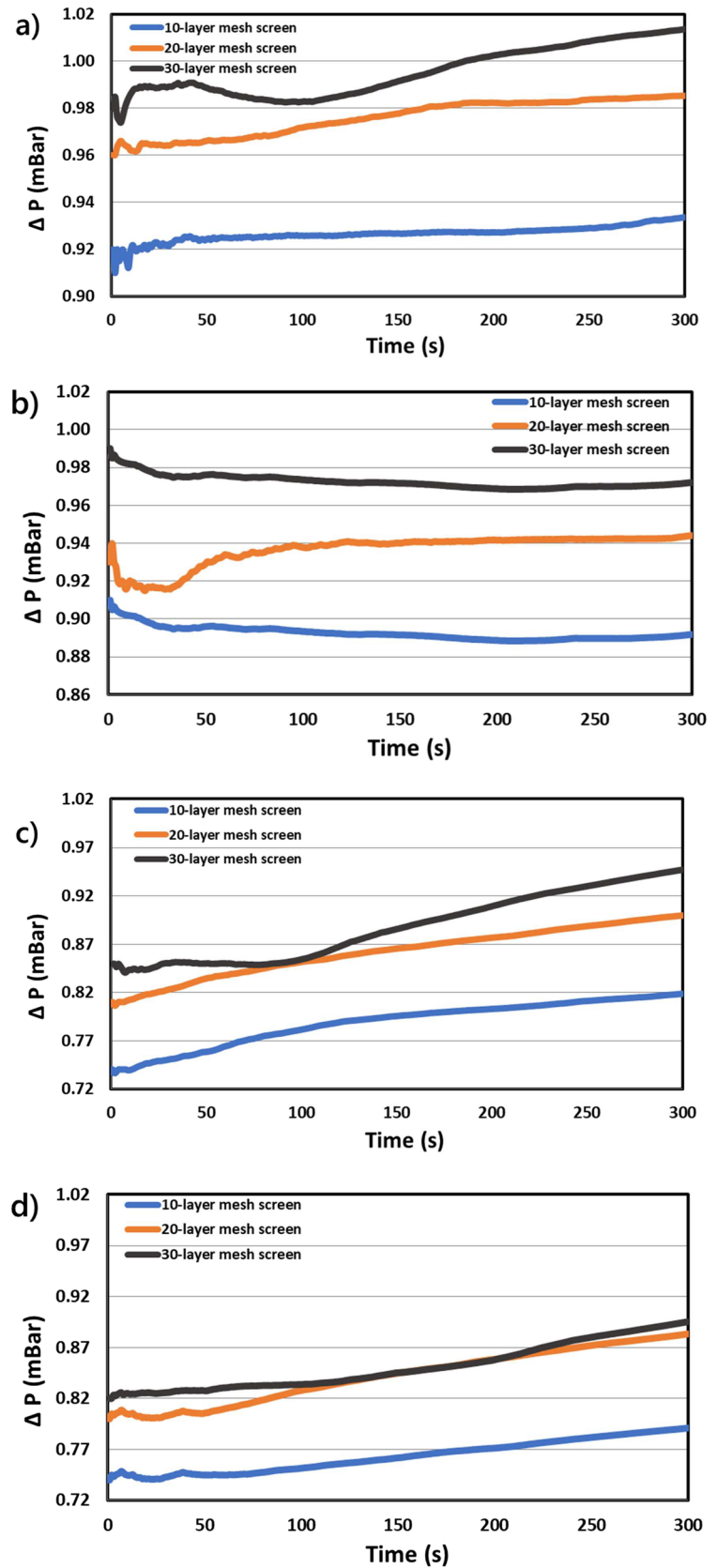
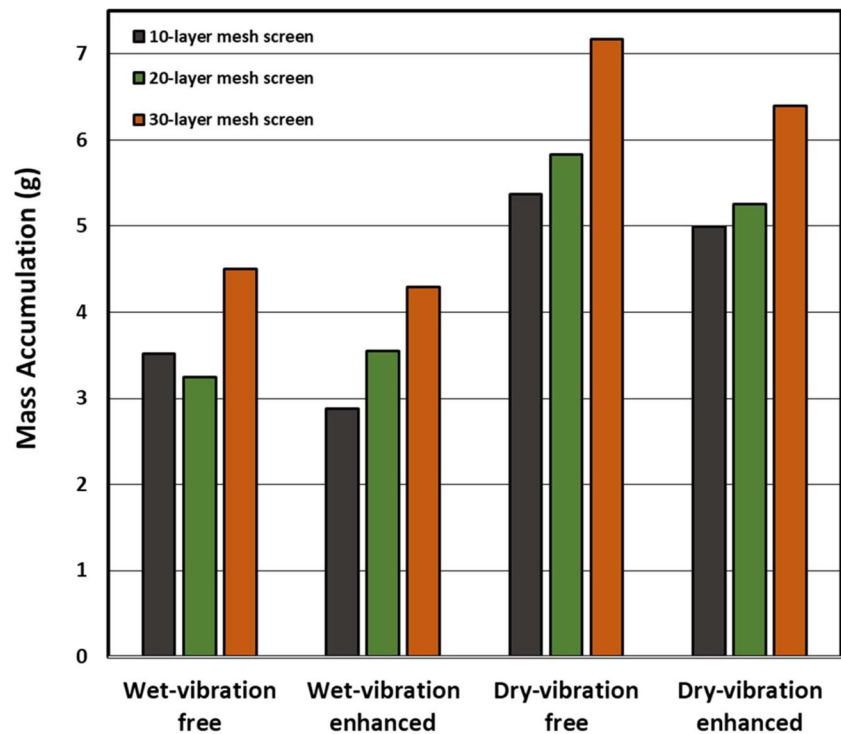


Fig. 10 Mass accumulation on mesh screen with different layering under various operational modes



is the test performed under the wet vibrating operational condition performed with a 20-layer filter.

These results correlate well with a study conducted by Sczap et al. [51] which investigated the clogging of a flood-bed scrubber filter panel both experimentally and theoretically. The results indicated that the pressure drop evolved differently with the pore structure of the filter medium. In addition, the pressure drop increased with dust accumulation within the filter [51]. Increasing the density of the filter media results in increased dust accumulation within the mesh screen panel, which increases the pressure drop across the mesh screen.

The surface of the filter panels can be coated in different ways to increase wettability and enhance particle-liquid adhesion. Following the protocols explained in Section 2.2, super hydrophobic filter coatings were obtained using a commercial polymer agent using the application instructions provided by the vender. Alternatively, the hydrophilic filters were obtained by heating them in a high-temperature low-oxygen environment furnace at 750 °C for 20 min, allowing the formation of a blue magnetite layer on the surface of the stainless-steel filter.

Data from these tests are shown in Figs. 11, 12, 13, and 14 and include measurement of both dust collection efficiency and clogging mitigation. First, Fig. 11 shows the dust collection efficiency for the specified operational conditions. Across all conditions, the hydrophilic surfaces imparted the highest collection efficiency, with the differences being more pronounced for the vibration-free

conditions as opposed to the vibration-enhanced conditions.

Air velocity loss data for the tested operational conditions are shown in Fig. 12. As anticipated, the dry conditions showed the highest air velocity loss, and in all cases, the hydrophilic mesh outperformed the other two. Overall, this data follows the same trend as that of collection efficiency with the difference between the various treatments being more pronounced in the vibration-free cases.

Similarly, Fig. 13 shows the real time pressure drop data through the test duration. For the wet condition tests, the pressure drop was similar for all three surface treatments; however, significant deviations were observed in the dry tests. Generally, the hydrophilic and bear meshes performed similarly, with the hydrophobic mesh exhibiting a significantly higher pressure drop.

Lastly, the mass of particle accumulation on the filter, which is another parameter that indicates the clogging process of the mesh screen and shows the self-cleaning capacity of the filter, was examined. Data from this analysis is shown in Fig. 14 and closely follows the trends of air velocity loss shown in Fig. 12.

When the tests carried out under various operational conditions with different surface modifications are examined together, hydrophobic surface modifications tended to reduce system efficiency relative to the baseline, while hydrophilic treatment tended to improve conditions. These results closely align with those of the laboratory testing and validate the approach employed in that section. In

Fig. 11 Collection efficiency by different mesh screens with various surface treatments under various operational modes

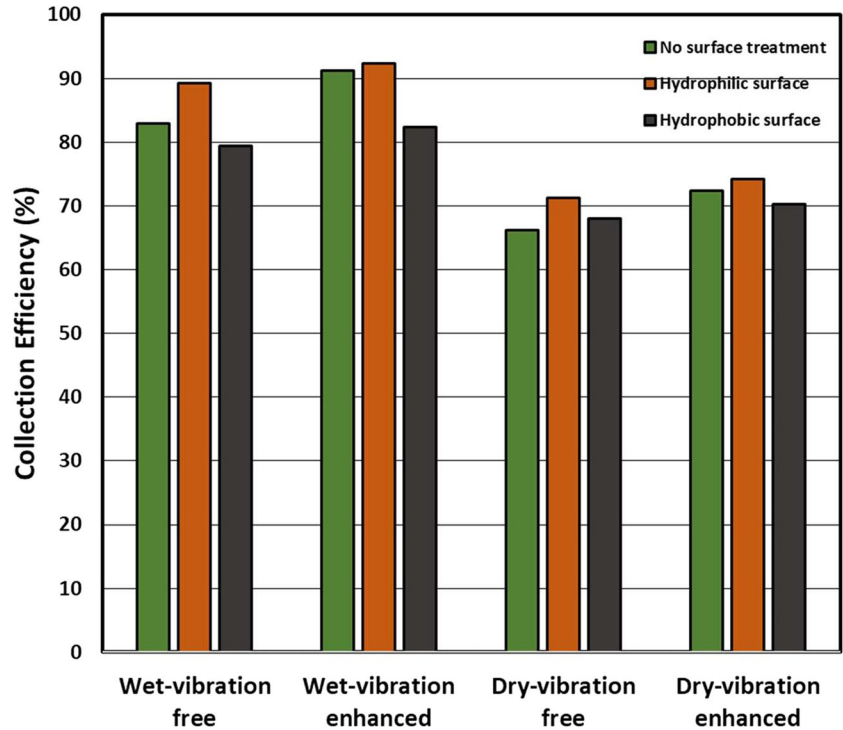
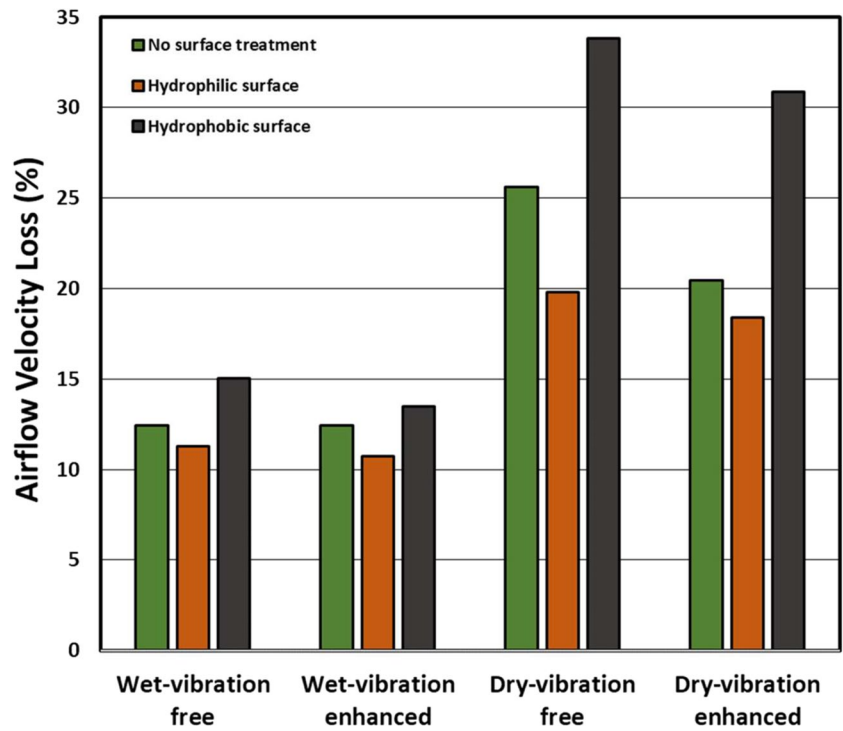


Fig. 12 Downwind section air velocity loss on mesh screen with different surface treatment applications under various operational modes



explaining the findings, when water contacts hydrophilic surfaces, it forms a film, whereas when it contacts hydrophobic surfaces, it beads up. Since water droplets are highly mobile, if the surface becomes hydrophobic, the area covered by water droplets is significantly reduced

of the total mesh wire surface area. Besides, hydrophilic coating is increasing the amount of liquid surface area on mesh, which increases chances of dust particles getting captured by the water droplets.

Fig. 13 Δp across mesh screen with different surface treatments of **a** wet and vibration-free mode, **b** wet and vibration mode, **c** dry and vibration-free mode, and **d** dry and vibration mode

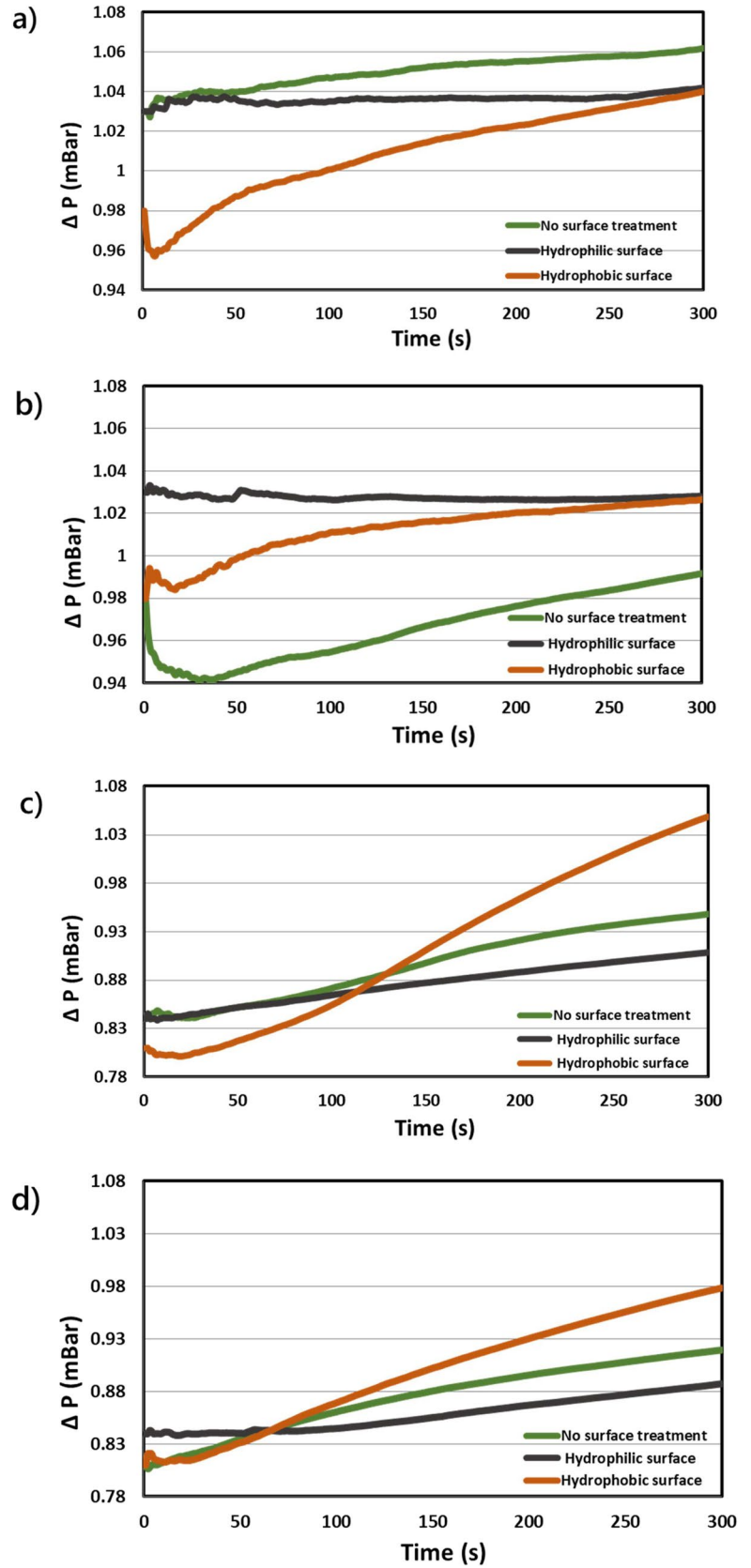
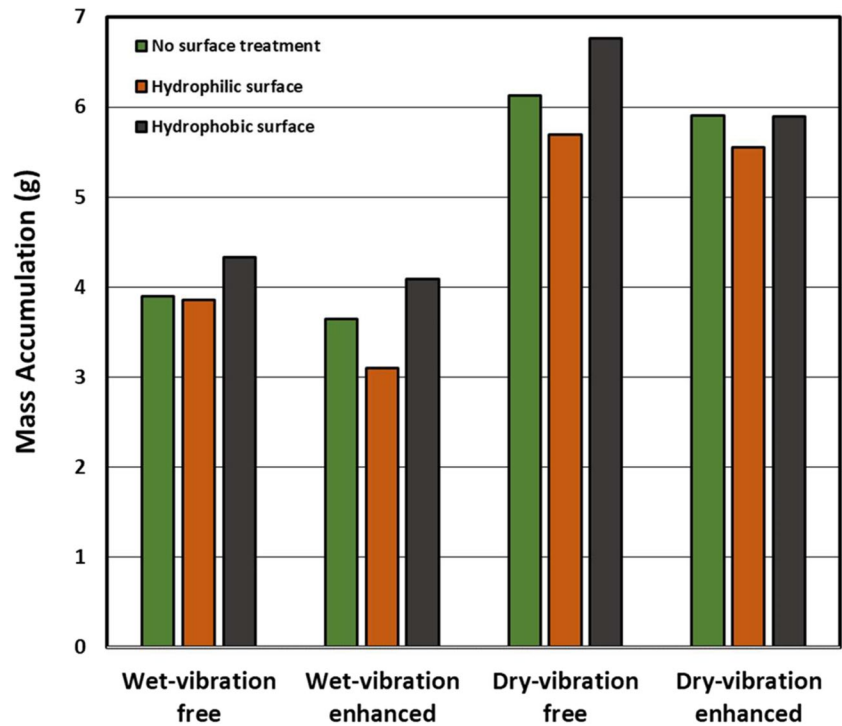


Fig. 14 Mass accumulation on mesh screen with different surface treatments under various operational modes



The final portion of the study utilized a three-factor Box-Behnken design (BBD) to examine the combinatory effects of mesh design, surface modifications, and vibrational frequency on system performance. The factors and levels associated with the independent variables are listed in Table 1. In total, 15 tests were carried out with different combinations of the variables. To determine the size distributions of the dust removed by the filter, upwind and downwind dust samples were analyzed using a Microtrac S3500 laser particle size analyzer.

Response surface plots were created with the results and are shown in Figs. 15, 16, 17, 18, and 19. Each figure shows the effect of two different variables on response by keeping one of the three variables used during the experiment constant. The collection efficiency surface (Fig. 15) was plotted from the data obtained with the gravimetric sampling. In Fig. 15a, the effect of the interaction of the filter density with the surface treatment on the efficiency is examined. The highest efficiencies (over 90%) were obtained when the filter frame filled with 30-layer, and at the same time

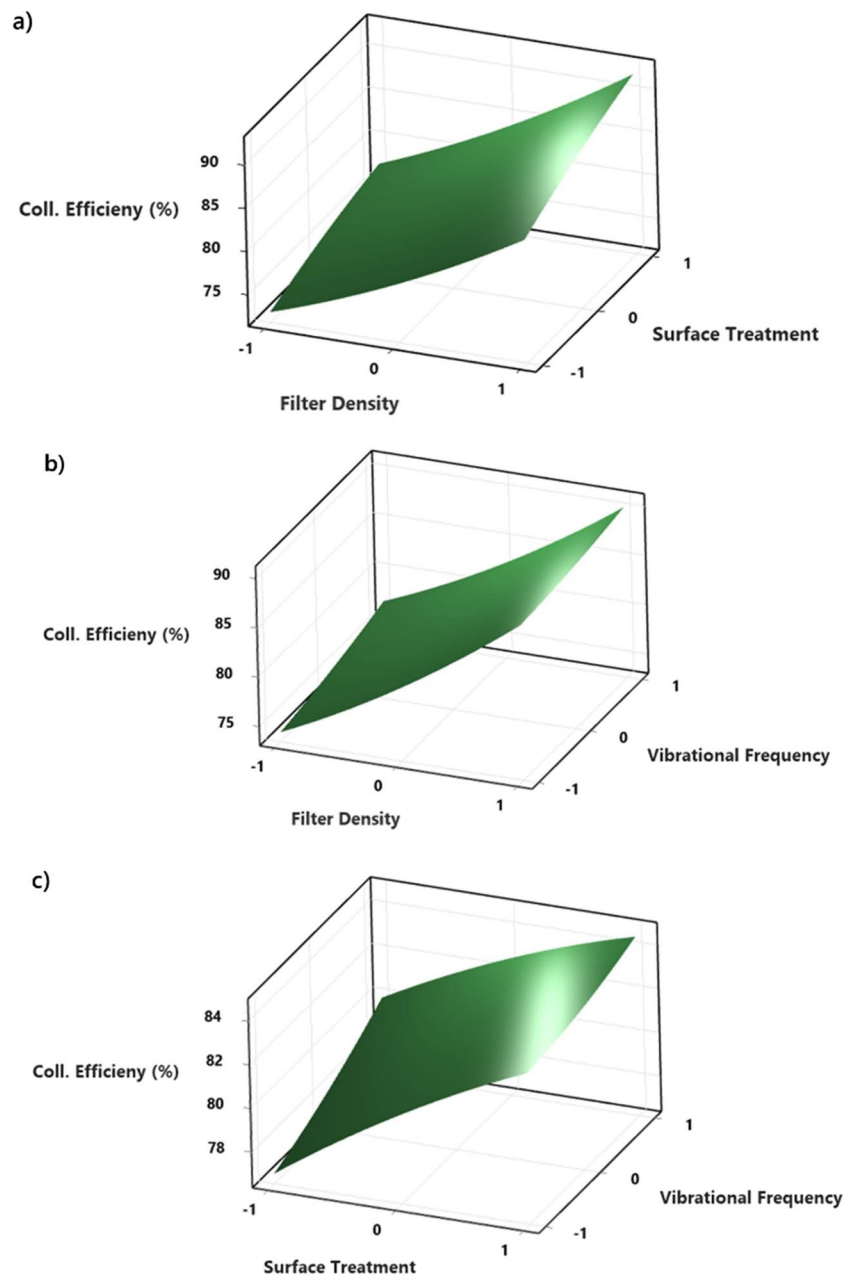
the mesh surface was hydrophilic. The effect of the interaction of the filter density with the frequency on the efficiency shown examined in Fig. 15b. The highest efficiency values (over 90%) were obtained when the filter frame filled with 30-layer. Fig. 15c shows the combinatory effects of vibrational frequency and surface modification. Compared to the filter density and surface modifications, the frequency had little impact on the collection efficiency. However, it is worth noting that the collection efficiencies approached maximum levels under the conditions where the densest hydrophilic filter excited with 134 Hz.

In Fig. 16, the effects of the binary interactions of the variables used in the test on the air velocity lost during the test were examined. In Fig. 16a where the effect of the filter density with the surface treatment pair on air velocity loss is examined, the data shows that the air velocity loss is most pronounced (over 1.4 m/s) when the filter density is at its densest level (30-layer), and when the hydrophobic coating was applied to the mesh screen. Fig. 16b shows that the air velocity loss reaches the highest levels with the 30-layer

Table 1 Independent variables and their respective values

Factors	Level		
	Low (-1)	Medium (0)	High (+1)
Filter density (layering)	10-layer	20-layer	30-layer
Surface treatment	Hydrophobic treatment	No surface treatment	Hydrophilic treatment
Frequency (Hz)	0	67	134

Fig. 15 Surface plots of collection efficiency (%) vs **a** filter density (−1: 10-layer, 0: 20-layer, +1: 30-layer) and surface treatment (−1: hydrophobic, 0: bare surface, +1: hydrophilic), **b** filter density (−1: 10-layer, 0: 20-layer, +1: 30-layer) and frequency (−1: 0 Hz, 0: 67 Hz, +1: 134 Hz), and **c** surface treatment (−1: hydrophobic, 0: bare surface, +1: hydrophilic) and frequency (−1: 0 Hz, 0: 67 Hz, +1: 134 Hz)

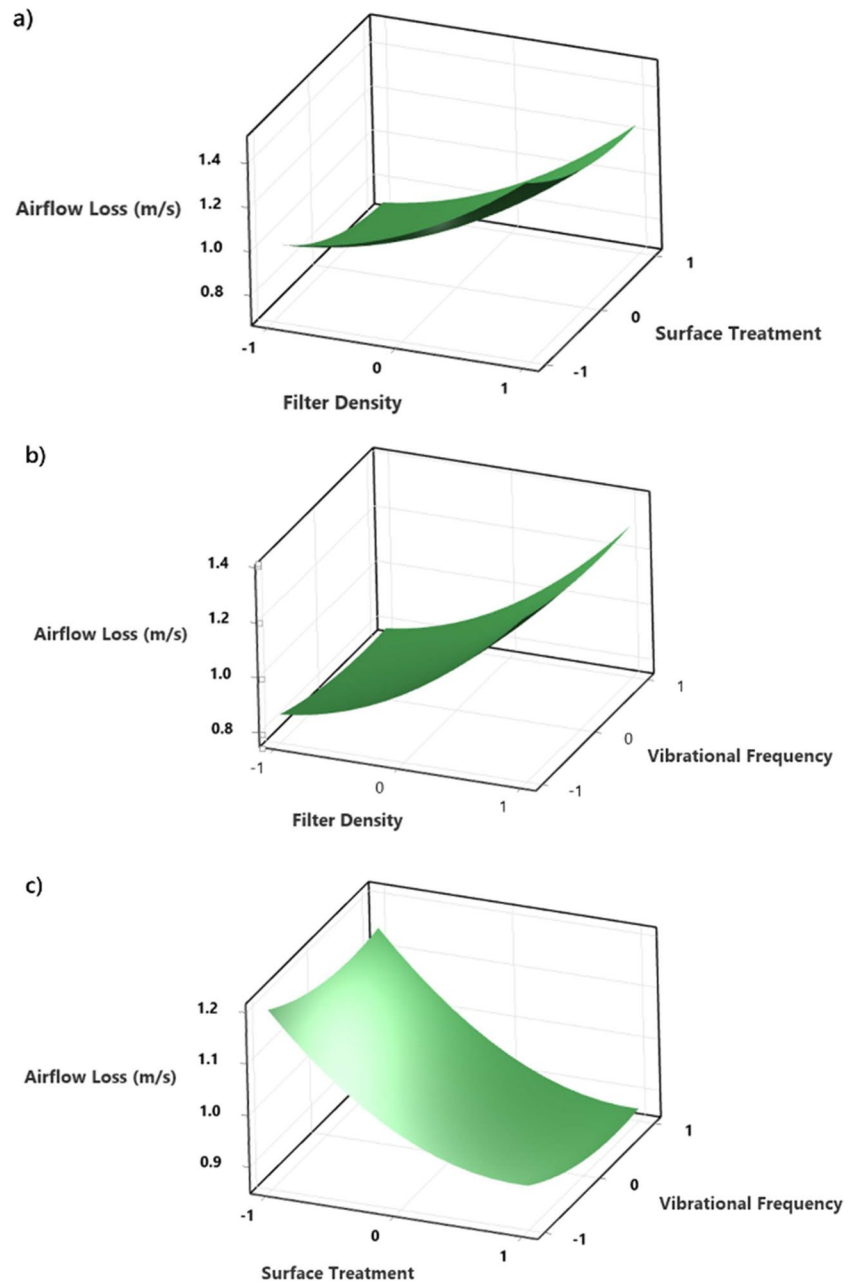


mesh screen in a vibration-free environment. Similarly, the hydrophobic surface modification increases the air velocity losses by over 1.2 m/s in a vibration-free environment. Altogether, the data show that air velocity loss can be minimized by using hydrophilic mesh screen package with lower mesh density and when vibrating the mesh screen around 134 Hz. Additionally, Fig. 17 shows the effect of the binary interactions of the variables used in the experimental design on the pressure drops across the mesh screen. As Bernoulli's equation defines, the changes in the pressure drop between upstream and downstream in a chamber and the air velocity in the system are directly related. Thus, the increases in pressure drop tended to be similar to the losses in air velocity. A

30-layer hydrophobic filter tested in a vibration-free environment produced the greatest increase in pressure drop. The least increase in pressure difference was found with the highest frequency value (134 Hz) and the least dense (10-layer) hydrophilic filter package.

To determine the self-cleaning capacity of the mesh screen, the amount of mass accumulations within the figure was measured after each test. Figure 18 shows the data from this analysis. As anticipated from the pressure drop data, the static test with a 30-layer mesh screen and increased hydrophobicity yielded the highest mass accumulation (over 4.8 g collected over a 5-min test). Under the conditions tested, frequency did not have a significant

Fig. 16 Surface plots of upstream air velocity loss (m/s) vs **a** filter density (−1: 10-layer, 0: 20-layer, +1: 30-layer) and surface treatment (−1: hydrophobic, 0: bare surface, +1: hydrophilic), **b** filter density (−1: 10-layer, 0: 20-layer, +1: 30-layer) and frequency (−1: 0 Hz, 0: 67 Hz, +1: 134 Hz), and **c** surface treatment (−1: hydrophobic, 0: bare surface, +1: hydrophilic) and frequency (−1: 0 Hz, 0: 67 Hz, +1: 134 Hz)

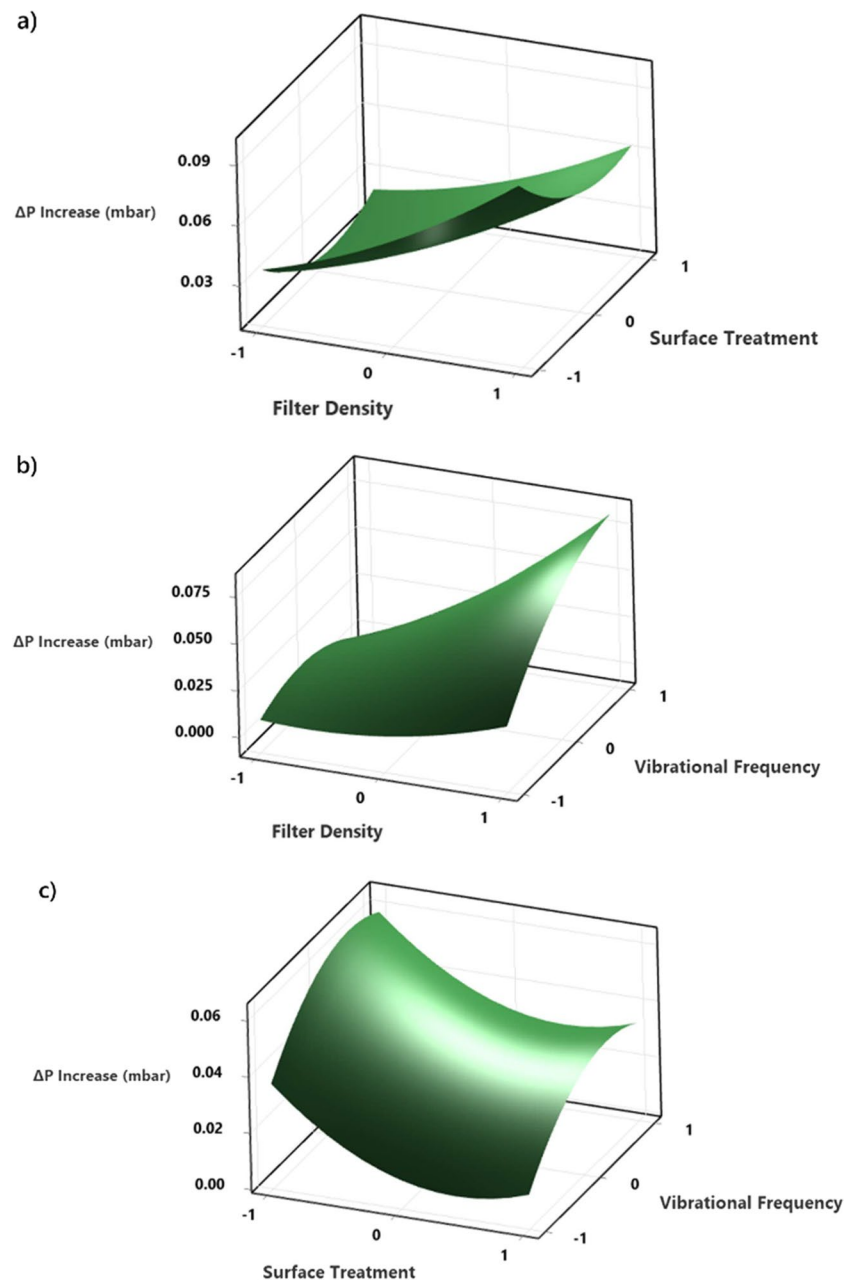


effect on the dust accumulation (Fig. 18b); however, a hydrophilic mesh combined with vibration was shown to be most effective, accumulating less than 3 g over the test period.

Lastly, Fig. 19 shows the interaction between vibration, filter density, and surface treatment in the reduction of fine respirable dust material ($-2.5 \mu\text{m}$). In Fig. 19a, the test with a hydrophobic mesh screen shows the lowest values for respirable material reduction (below 60%), regardless of the number of layers in the filter pack. In contrast, when all figures are combined, when the surface is hydrophilic and the filter thickness is 30-layer, the amount of respirable substances eliminated increases by over 80%.

These results compare well with a study by Sczap et al. (2023) which reports that mesh design and surface hydrophobicity significantly impact the clogging rate of the filter in an FBS. Decreasing the contact angle of the mesh screen surface improves the system performance and extends the life of the filter panel by preventing rapid mass accumulation within the filter. This application reduces hydrophobicity, increases wetting, and improves filtration efficiency. Steel woven filters inherently possess some level of hydrophobicity, causing them to repel water to some extent. By decreasing the contact angle, this hydrophobic behavior is diminished, allowing the mesh screen to attract water more effectively. Consequently, the surface becomes

Fig. 17 Surface plots of pressure drop across the mesh screen (mbar) vs **a** filter density (−1: 10-layer, 0: 20-layer, +1: 30-layer) and surface treatment (−1: hydrophobic, 0: bare surface, +1: hydrophilic), **b** filter density (−1: 10-layer, 0: 20-layer, +1: 30-layer) and frequency (−1: 0 Hz, 0: 67 Hz, +1: 134 Hz), and **c** surface treatment (−1: hydrophobic, 0: bare surface, +1: hydrophilic) and frequency (−1: 0 Hz, 0: 67 Hz, +1: 134 Hz)

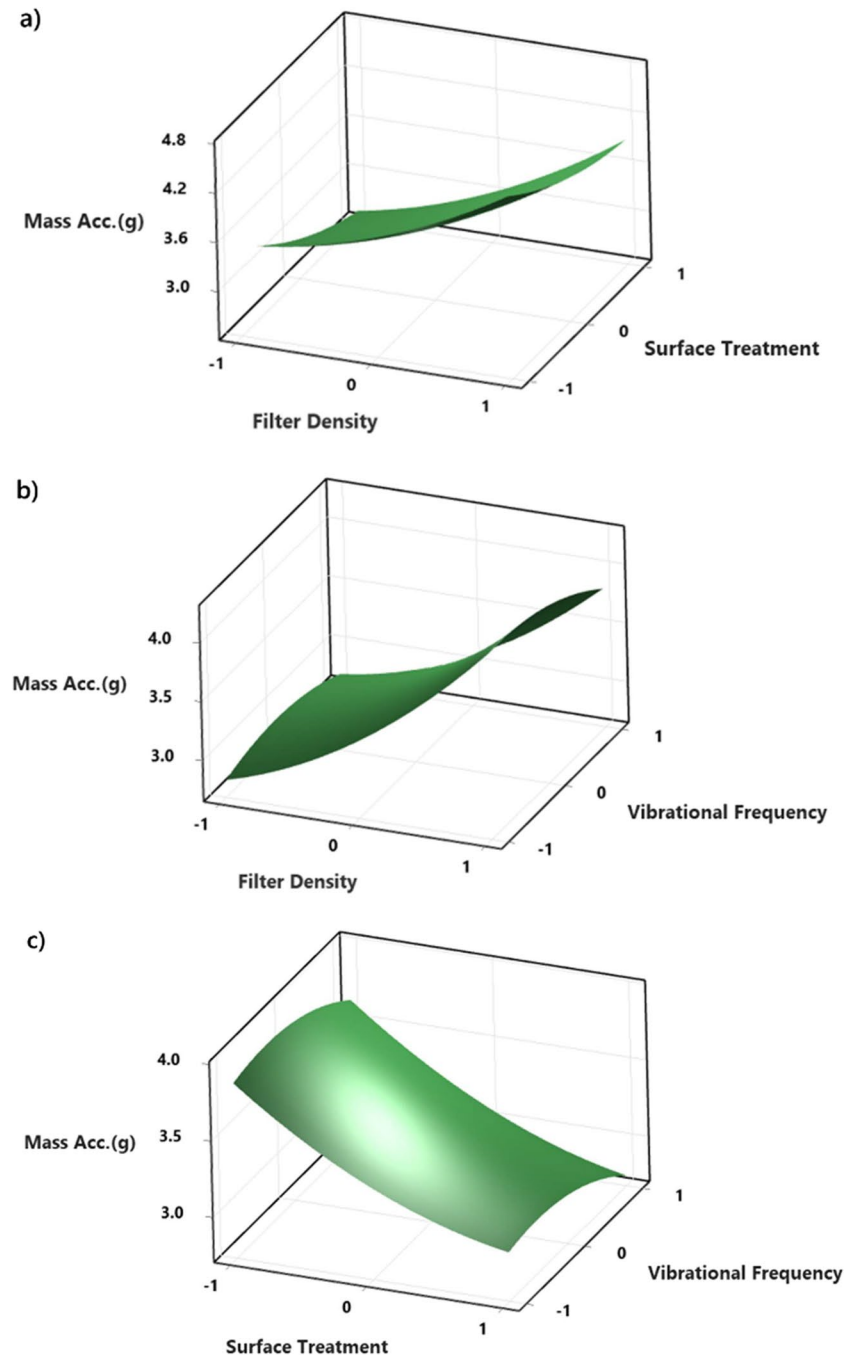


more wettable, enabling water droplets to spread more easily across it. The primary purpose of the mesh screen is to serve as a medium for water droplets to interact with dust particulates and capture them. Decreasing the contact angle of the surface enhances the interaction between the screen surface and water droplets. This, in turn, fosters better contact between the filter surface and dust particles suspended in the water, potentially enhancing the system's efficiency in capturing dust particles.

Additionally, as mesh screen package thickness increases, dust particles accumulate more rapidly within the filter panel, increasing pressure drop and lowering

system performance [51]. Inversely, as the filter media density decreases, more void areas appear within the filter media. As a result, some dust material passes through the mesh panel without being captured by water droplets. The less dense filter media does not offer better dust collection efficiency for this reason. The hydrophilic and vibrationally enhanced mesh screen, however, sustains more airflow through the system, slows the increase in pressure drop, and improves mass retention within the filter. Therefore, less dense hydrophilic and vibrating mesh screen panels can outperform higher-density panels for longer periods of time.

Fig. 18 Surface plots of mass retain within the mesh screen (g) vs **a** filter density (−1: 10-layer, 0: 20-layer, +1: 30-layer) and surface treatment (−1: hydrophobic, 0: bare surface, +1: hydrophilic), **b** filter density (−1: 10-layer, 0: 20-layer, +1: 30-layer) and frequency (−1: 0 Hz, 0: 67 Hz, +1: 134 Hz), and **c** surface treatment (−1: hydrophobic, 0: bare surface, +1: hydrophilic) and frequency (−1: 0 Hz, 0: 67 Hz, +1: 134 Hz)

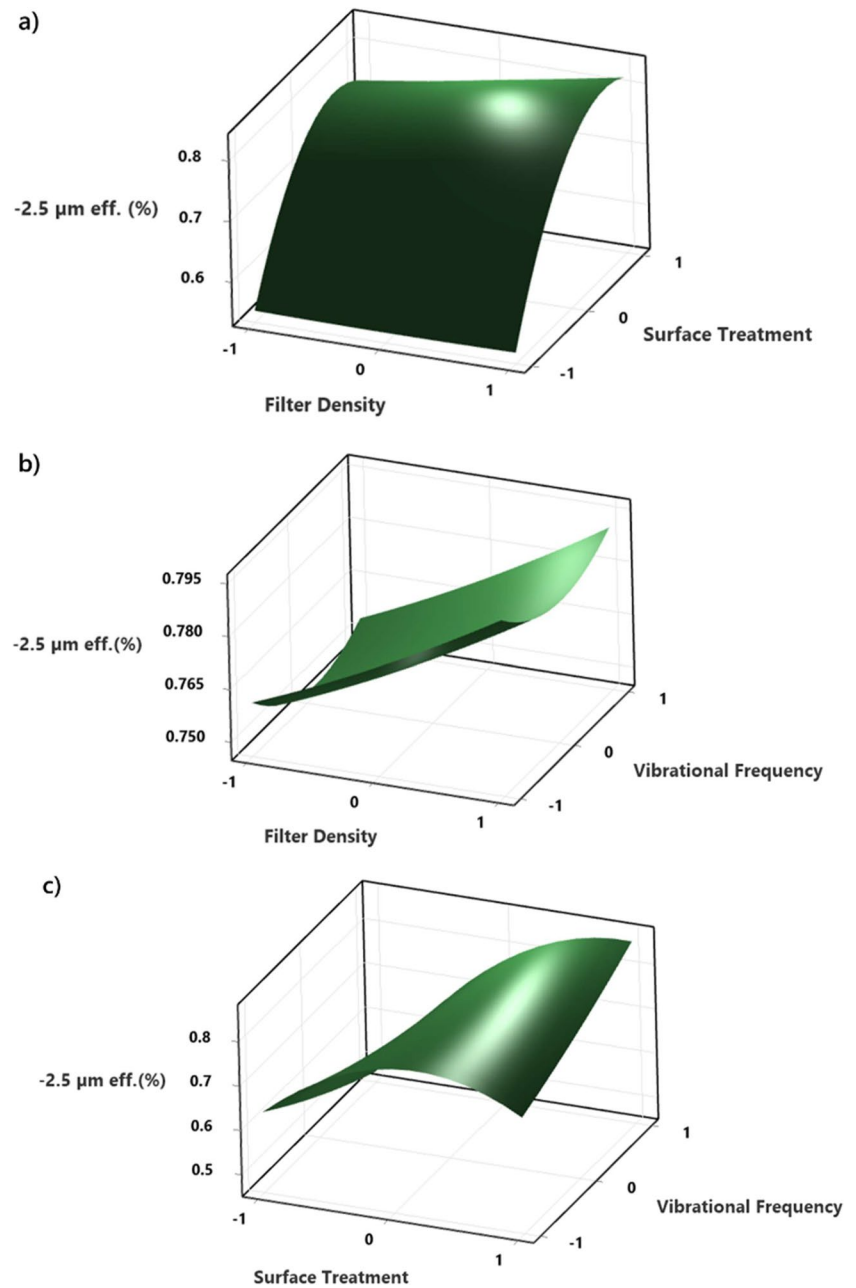


4 Conclusion and Summary

Flooded bed dust scrubbers utilized in underground mining operations are particularly susceptible to clogging. As dirty areas in the mesh become loaded with particles, the pressure drop across the screen increases, resulting in reduced airflow volumes and lower overall air cleaning efficiency. Thus, one way to improve overall system efficiency is to continuously remove particles from congested regions, which allows the system to maintain higher interior airflow rates. In this study,

modifications to the filter surface and mesh thicknesses were examined to determine their combined effect on vibration-enhanced flooded bed dust scrubber performance. Tests were performed in laboratory-scale scrubber unit using mesh screens with different surface treatments and filter media densities. The effects of various factors were measured in both a wet and dry environment, as well as with and without vibrations. As part of the tests, air velocity, pressure drop, and the weight of dust particles accumulated inside the mesh screen were measured.

Fig. 19 Surface plot reduction in respirable size (%) vs **a** filter density (−1: 10-layer, 0: 20-layer, +1: 30-layer) and surface treatment (−1: hydrophobic, 0: bare surface, +1: hydrophilic), **b** filter density (−1: 10-layer, 0: 20-layer, +1: 30-layer) and frequency (−1: 0 Hz, 0: 67 Hz, +1: 134 Hz), and **c** surface treatment (−1: hydrophobic, 0: bare surface, +1: hydrophilic) and frequency (−1: 0 Hz, 0: 67 Hz, +1: 134 Hz)



Overall, the results confirm the benefit of a vibrating mesh FBS, as has been demonstrated in prior studies [27, 34, 35]. Moreover, the results show that the system can be further optimized through control of the mesh density and particularly the mesh hydrophobicity. Results with different mesh thicknesses generally confirm prior studies showing that higher mesh density increased dust collection; however, it also shows higher clogging potential as demonstrated through both mass accumulation and pressure drop. Interestingly, testing with different mesh surface modifications showed that optimal results were obtained with hydrophilic mesh surface, which exhibited reduced clogging but similar dust collection as compared to the hydrophobic and

untreated counterparts. In summary, the results showed that the system performance can be optimized when using hydrophilic 20- or 30-layer filters that are excited by frequencies between 67 and 134 Hz. These benefits were most notable in the −2.5 micron size class, where proper optimization of the mesh frequency, mesh wettability, and mesh density can lead to nearly 30% increases in fine dust removal. Ultimately, this study provides a substantial contribution to the understanding of mesh design, surface modifications, and vibrational effects in shaping dust scrubber system efficiency.

Acknowledgements The authors would like to acknowledge Matt Shigo's assistance in designing and manufacturing the test setup,

Brian Arnold's help in testing, and John Sczap's assistance in providing the laboratory procedure for surface preparation and contact angle measurements.

Funding This study was sponsored by the Alpha Foundation for the Improvement of Mine Safety and Health, Inc. (Alpha Foundation).

Declarations

Competing Interests The authors declare no competing interests.

Disclaimer The views, opinions, and recommendations expressed herein are solely those of the authors and do not imply any endorsement by the Alpha Foundation, its directors, and staff.

Open Access This article is licensed under a Creative Commons Attribution 4.0 International License, which permits use, sharing, adaptation, distribution and reproduction in any medium or format, as long as you give appropriate credit to the original author(s) and the source, provide a link to the Creative Commons licence, and indicate if changes were made. The images or other third party material in this article are included in the article's Creative Commons licence, unless indicated otherwise in a credit line to the material. If material is not included in the article's Creative Commons licence and your intended use is not permitted by statutory regulation or exceeds the permitted use, you will need to obtain permission directly from the copyright holder. To view a copy of this licence, visit <http://creativecommons.org/licenses/by/4.0/>.

References

- IARC (1997) Silica, some silicates, coal dust and para-aramid fibrils. IARC monographs on the evaluation of carcinogenic risks to humans, No. 68, IARC working group on the evaluation of carcinogenic risks to humans. International agency for research on cancer, Lyon
- ISO. International Organization for Standardization (1995) Air quality - particle size fraction definitions for health-related sampling 7708:1995
- Occupational Safety and Health Administration (2010) Occupational exposure to respirable crystalline silica—review of health effects literature and preliminary quantitative risk assessment, Washington
- World Health Organization, Environment, Climate Change and Health Team (1999) Hazard prevention and control in the work environment: airborne dust. WHO/SDE/OEH/99.14
- Castranova V, Vallyathan V (2000) Silicosis and coal workers' pneumoconiosis. *Environ Health Perspect* 108(Suppl. 4):675–684
- Vincent JH (1999) Particle size-selective sampling of particulate air contaminants, American conference of governmental industrial hygienists, health & environmental research online (HERO) 13243
- Mischler SE, Cauda EG, Di Giuseppe M, McWilliams LJ, Croix CS, Sun M, Franks J, Ortiz LA (2016) Differential activation of RAW 264.7 macrophages by size-segregated crystalline silica. *J Occup Med Toxicol* 11(1):57. <https://doi.org/10.1186/s12995-016-0145-2>
- Colinet J, Listak JM, Organiscak JA, Rider JP, Wolfe AL (2010) Best practices for dust control in coal mining, Department of Health and Human Services, Centers for Disease Control and Prevention. National Institute for Occupational Safety and Health, Office of Mine Safety and Health Research
- Sapko MJ, Cashdollar KL, Green GM (2007) Coal dust particle size survey of US mines. *J. Loss Prev. Process Ind.* 20:616–620. <https://doi.org/10.1016/j.jlp.2007.04.014>
- Thomas Sporn VR (2013) Consideration of occupational lung disease and pneumoconiosis in forensic pathology. *Acad Forensic Pathol* 3(4):370–385
- MSHA (2016) Respirable dust standards, 30 CFR § 70.100
- Centers for Disease Control (CDC) (2006) Advanced cases of coal workers' pneumoconiosis—two counties, Virginia. *MMWR* 55:33
- National Institute for Occupational Safety and Health, DHHS (NIOSH) (1995) Criteria for a recommended standard: occupational exposure to respirable coal mine dust 95–106
- Suarthana E, Laney AS, Storey E, Hale JM, Attfield MD (2011) Coal workers' pneumoconiosis in the United States: regional differences 40 years after implementation of the 1969 Federal Coal Mine Health and Safety Act. *Occup Environ Med* 68:908–913. <https://doi.org/10.1136/oem.2010.063594>
- Blackley DJ, Halldin CN, Laney AS (2014) Resurgence of a debilitating and entirely preventable respiratory disease among working coal miners. *Am J Respir Crit Care Med.* <https://doi.org/10.1164/rccm.201407-1286LE>
- U.S. Department of Labor (2014) Final rule. <http://arlweb.msha.gov/regs/fedreg/final/2014finl/2014-09084.asp>. Accessed June 5, 2022.
- Wang W, Peng FF (1991) Analyses of respirable dust distributions with multiple dust sources on longwall faces. In: Proceedings of society for mining, metallurgy & exploration, 367–375
- Colinet JF, Spencer ER, Jankowski RA (1997) Status of dust control technology on U.S. longwalls. In: Proceedings of 6th International Mine Ventilation Congress, pp 345–351
- Arya S, Sottile J, Novak T (2018) Development of a flooded-bed scrubber for removing coal dust at a longwall mining section. *Saf Sci* 110:204–213. <https://doi.org/10.1016/j.ssci.2018.08.003>
- Arya S, Sottile J, Rider JP, Colinet JF, Novak T, Wedding C (2018) Design and experimental evaluation of a flooded-bed dust scrubber integrated into a longwall shearer. *Powder Technol* 339:487–496. <https://doi.org/10.1016/j.powtec.2018.07.072>
- Arya S, Novak T, Saito K et al (2019) Empirical formulae for determining pressure drop across a 20-layer flooded-bed scrubber screen. *Min Metall Explor* 36(6):1169–1177. <https://doi.org/10.1007/s42461-019-0091-5>
- Arya S (2018) Investigation of the effectiveness of an integrated flooded-bed dust scrubber on a longwall shearer through laboratory testing and CFD simulation. Doctoral Dissertation, Mining Engineering, University of Kentucky. <https://doi.org/10.13023/ETD.2018.074>
- Reed W, Taylor C (2007) Factors affecting the development of mine face ventilation systems in the 20th century. SME annual meeting and exhibit 07–071
- Cowley SR, McCoy BS (1993) Wet scrubber apparatus. U.S. Patent No. 5,178,654, Washington, DC, U.S. Patent and Trademark Office
- Campbell JA, Moynihan DJ, Roper WD, Willis EC (1983) Dust control system and method of operation. Patent Number US 4380353
- Colinet JF, Jankowski RA (2000) Silica collection concerns when using flooded-bed scrubbers. *Min Eng* 52(4):49–54
- Uluer ME, Shigo M, Amini SH, Noble A (2023) An exploratory investigation on the effectiveness of a novel vibration-enhanced flooded bed dust scrubber. *Min Metall Explor*:2524–3470. <https://doi.org/10.1007/s42461-023-00889-w>
- Colinet J, Reed WR, Potts JD (2013) Impact on respirable dust levels when operating a flooded-bed scrubber in 20-foot cuts. Office for mine safety and health research. Report of investigations (National institute for occupational safety and health) 9693

29. National Institute for Occupational Safety and Health (2002) Exposure to silica dust on continuous mining operations using flooded-bed scrubbers. *Appl Occup Environ Hyg* 17(5):322–323. <https://doi.org/10.1080/10473220252864888>
30. Salazar AJ, Saito K, Alloo RP, Tanaka N (2000) Wet scrubber and paint spray booth including the wet scrubber. US Patent 6, 093, 250
31. Kumar AR, Schafrik S (2020) Multiphase CFD modeling and laboratory testing of a Vortecone for mining and industrial dust scrubbing applications. *Process Saf Environ Prot* 144:330–336. <https://doi.org/10.1016/j.psep.2020.07.046>
32. Taylor A, Schafrik S, Kumar AR (2019) The Vortecone: a new maintenance-free wet scrubber device. Future Mining, Sydney, NSW
33. Kumar AR, Schafrik S, Velasquez O (2020) Designing, modeling, and laboratory testing of a non-clogging impingement type filter for mining dust scrubbers. *Min Metall Explor* 37(6):1911–1918. <https://doi.org/10.1007/s42461-020-00311-9>
34. Lu Z, Rath A, Amini SH, Noble A, Shahab S (2022) A computational fluid dynamics investigation of a novel flooded-bed dust scrubber with vibrating mesh. *Int J Min Sci Technol* 32(3):525–537. <https://doi.org/10.1016/j.ijmst.2022.03.002>
35. Janjua AN, Shaefer M, Amini SH, Noble CA, Shahab S (2024) Vibrational energy transmission in underground continuous mining: dynamic characteristics and experimental research of field data. *Appl Energy* 354(Part A):122220. <https://doi.org/10.1016/j.apenergy.2023.122220>
36. King RP (2001) Classification based on sieving–vibrating screens. In: *Modeling and simulation of mineral processing systems*. Elsevier, pp 81–86
37. Chen Z, Zhou Z, Peng J (2022) Dust removal mechanism of the vibrating string filter with charged water mist. *Int J Rotating Mach* 2022. <https://doi.org/10.1155/2022/5713983>
38. Mishin IF, El'bert EI, Belikov VI, Tumanov AN, Kachaev VK (1975) Cleaning coal tar by vibrating–screen filtration, surfactant treatment, and short-term clarification. *Coke Chem USSR* 4:32–35
39. Yang X, Wang H, Chase GG (2015) Performance of hydrophilic glass fiber media to separate dispersed water drops from ultra low sulfur diesel supplemented by vibrations. *Sep Purif Technol* 156:665–672. <https://doi.org/10.1016/j.seppur.2015.10.062>
40. Kim SC, Wang H, Imagawa M, Chen DR, Pui DY (2006) Experimental and modeling studies of the stream-wise filter vibration effect on the filtration efficiency. *Aerosol Sci Technol* 40(6):389–395. <https://doi.org/10.1080/02786820600640541>
41. Genkin G, Waite TD, Fane AG, Chang S (2006) The effect of vibration and coagulant addition on the filtration performance of submerged hollow fibre membranes. *J Membr Sci* 281(1-2):726–734. <https://doi.org/10.1016/j.memsci.2006.04.048>
42. Nițoi D, Amza G, Amza Z, Radu C, Teodorescu M (2018) Practical realisation and finite element modeling of ultrasonic filters design for air filtration. *Int Multidiscip Sci GeoConf: SGEM* 18(4.2):555–562. <https://doi.org/10.1088/1757-899X/400/2/022003>
43. Fuchs EP (1979) Coal mining equipment vibration data report. Donaldson Company, Inc.
44. Shahab S (2015) Vibration energy harvesting, biomimetic actuation, and contactless acoustic energy transfer in a quiescent fluid domain. George W. Woodruff school of mechanical engineering, college of engineering, georgia institute of technology, dissertation.
45. Colinet J, Halldin CN, Schall J (2021) Best practices for dust control in coal mining, second edition. National Institute of Occupational Safety and Health, Pittsburgh, PA; Spokane, WA. <https://doi.org/10.26616/NIOSHPUB2021119>
46. Chander S, Alaboyun AR, Aplan FF, Section MP (1990) On the mechanism of capture of coal dust particles by sprays. In: *Proceedings of the 3rd symposium on respirable dust in the mineral industries, society for mining, metallurgy, and exploration Inc* p 193–202
47. Tessum MW, Raynor PC (2017) Effects of spray surfactant and particle charge on respirable coal dust capture. *Saf Health Work* 8(3):296–305. <https://doi.org/10.1016/j.shaw.2016.12.006>
48. Kost JA, Shirey GA, Ford CT (1980) In-mine test for wetting agent effectiveness. Technical report, bituminous coal research, Inc, Bureau of mines, Washington
49. Kilau HW, Lantto OL, Olson KS, Myren TA, Voltz JI (1996) Stephen B. Thacker CDC library collection. Report of investigations (United States. Bureau of Mines) 9591
50. Szczap J, Pan L (2024) Understanding interfacial interactions in filter clogging of flooded bed scrubbers using experimental approach and modelling. Michigan technological university, Unpublished Manuscript
51. Szczap J, Jung S, Pan L (2024) Understanding the microscopic mechanism of clogging of both fibrous and mesh filters in flooded-bed wet scrubbers. *Fuel* 355:129381. <https://doi.org/10.1016/j.fuel.2023.129381>

Publisher's Note Springer Nature remains neutral with regard to jurisdictional claims in published maps and institutional affiliations.